Measurement of Branching Fractions, Isospin, and CP-Violating Asymmetries for Exclusive $b \to d\gamma$ Modes

N. Taniguchi,[19] M. Nakao,[9] S. Nishida,[9] I. Adachi,[9] H. Aihara,[46] K. Arinstein,[1] T. Aushev,[21,15] T. Aziz,[43] A. M. Bakich,[42] V. Balagura,[15] A. Bay,[21] K. Belous,[14] V. Bhardwaj,[36] U. Bitenc,[16] A. Bondar,[1] A. Bozek,[30] M. Bračko,[23,16] T. E. Browder,[8] M.-C. Chang,[4] P. Chang,[29] Y. Chao,[29] A. Chen,[27] K.-F. Chen,[29] W. T. Chen,[27] B. G. Cheon,[7] C.-C. Chiang,[29] I.-S. Cho,[51] Y. Choi,[41] J. Dalseno,[9] M. Dash,[50] A. Drutskoy,[3] W. Dungel,[13] S. Eidelman,[1] B. Golob,[22,16] H. Ha,[18] J. Haba,[9] T. Hara,[35] K. Hayasaka,[25] H. Hayashii,[26] M. Hazumi,[9] Y. Hoshi,[45] W.-S. Hou,[29] H. J. Hyun,[20] T. Iijima,[25] K. Inami,[25] A. Ishikawa,[38] H. Ishino,[47] R. Itoh,[9] M. Iwabuchi,[6] M. Iwasaki,[46] Y. Iwasaki,[9] N. J. Joshi,[43] D. H. Kah,[20] H. Kaji,[25] J. H. Kang,[51] H. Kawai,[2] T. Kawasaki,[32] H. Kichimi,[9] S. K. Kim,[40] Y. I. Kim,[20] Y. J. Kim,[6] K. Kinoshita,[3] S. Korpar,[16,23] P. Križan,[16,22] P. Krokovny,[9] R. Kumar,[36] A. Kuzmin,[1] Y.-J. Kwon,[51] S.-H. Kyeong,[51] J. S. Lange,[5] J. S. Lee,[41] S. E. Lee,[40] T. Lesiak,[30] A. Limosani,[24] S.-W. Lin,[29] C. Liu,[39] Y. Liu,[6] D. Liventsev,[15] F. Mandl,[13] S. McOnie,[42] K. Miyabayashi,[26] Y. Miyazaki,[25] G. R. Moloney,[24] Y. Nagasaka,[10] I. Nakamura,[9] E. Nakano,[34] H. Nakazawa,[27] Z. Natkaniec,[30] O. Nitoh,[49] T. Nozaki,[9] S. Ogawa,[44] T. Ohshima,[25] S. Okuno,[17] S. L. Olsen,[8,12] H. Ozaki,[9] P. Pakhlov,[15] G. Pakhlova,[15] C. W. Park,[41] H. Park,[20] H. K. Park,[20] K. S. Park,[41] L. S. Peak,[42] L. E. Piilonen,[50] H. Sahoo,[8] Y. Sakai,[9] N. Sasao,[19] O. Schneider,[21] J. Schümann,[9] C. Schwanda,[13] A. J. Schwartz,[3] R. Seidl,[11,37] K. Senyo,[25] M. E. Sevior,[24] M. Shapkin,[14] C. P. Shen,[12] J.-G. Shiu,[29] B. Shwartz,[1] J. B. Singh,[36] A. Sokolov,[14] S. Stanič,[33] M. Starič,[16] K. Sumisawa,[9] T. Sumiyoshi,[48] S. Y. Suzuki,[9] N. Tamura,[32] G. N. Taylor,[24] Y. Teramoto,[34] I. Tikhomirov,[15] K. Trabelsi,[9] T. Tsuboyama,[9] S. Uehara,[9] T. Uglov,[15] Y. Unno,[7] S. Uno,[9] P. Urquijo,[24] G. Varner,[8] C. H. Wang,[28] M.-Z. Wang,[29] P. Wang,[12] X. L. Wang,[12] Y. Watanabe,[17] R. Wedd,[24] J. Wicht,[21] E. Won,[18] B. D. Yabsley,[42] Y. Yamashita,[31] Y. Yusa,[50] Z. P. Zhang,[39] V. Zhilich,[1] V. Zhulanov,[1] T. Zivko,[16] A. Zupanc,[16] and O. Zyukova[1]

(Belle Collaboration)

[1]*Budker Institute of Nuclear Physics, Novosibirsk*
[2]*Chiba University, Chiba*
[3]*University of Cincinnati, Cincinnati, Ohio 45221*
[4]*Department of Physics, Fu Jen Catholic University, Taipei*
[5]*Justus-Liebig-Universität Gießen, Gießen*
[6]*The Graduate University for Advanced Studies, Hayama*
[7]*Hanyang University, Seoul*
[8]*University of Hawaii, Honolulu, Hawaii 96822*
[9]*High Energy Accelerator Research Organization (KEK), Tsukuba*
[10]*Hiroshima Institute of Technology, Hiroshima*
[11]*University of Illinois at Urbana-Champaign, Urbana, Illinois 61801*
[12]*Institute of High Energy Physics, Chinese Academy of Sciences, Beijing*
[13]*Institute of High Energy Physics, Vienna*
[14]*Institute of High Energy Physics, Protvino*
[15]*Institute for Theoretical and Experimental Physics, Moscow*
[16]*J. Stefan Institute, Ljubljana*
[17]*Kanagawa University, Yokohama*
[18]*Korea University, Seoul*
[19]*Kyoto University, Kyoto*
[20]*Kyungpook National University, Taegu*
[21]*École Polytechnique Fédérale de Lausanne (EPFL), Lausanne*
[22]*Faculty of Mathematics and Physics, University of Ljubljana, Ljubljana*
[23]*University of Maribor, Maribor*
[24]*University of Melbourne, School of Physics, Victoria 3010*
[25]*Nagoya University, Nagoya*
[26]*Nara Women's University, Nara*
[27]*National Central University, Chung-li*
[28]*National United University, Miao Li*
[29]*Department of Physics, National Taiwan University, Taipei*
[30]*H. Niewodniczanski Institute of Nuclear Physics, Krakow*
[31]*Nippon Dental University, Niigata*

[32]Niigata University, Niigata
[33]University of Nova Gorica, Nova Gorica
[34]Osaka City University, Osaka
[35]Osaka University, Osaka
[36]Panjab University, Chandigarh
[37]RIKEN BNL Research Center, Upton, New York 11973
[38]Saga University, Saga
[39]University of Science and Technology of China, Hefei
[40]Seoul National University, Seoul
[41]Sungkyunkwan University, Suwon
[42]University of Sydney, Sydney, New South Wales
[43]Tata Institute of Fundamental Research, Mumbai
[44]Toho University, Funabashi
[45]Tohoku Gakuin University, Tagajo
[46]Department of Physics, University of Tokyo, Tokyo
[47]Tokyo Institute of Technology, Tokyo
[48]Tokyo Metropolitan University, Tokyo
[49]Tokyo University of Agriculture and Technology, Tokyo
[50]Virginia Polytechnic Institute and State University, Blacksburg, Virginia 24061
[51]Yonsei University, Seoul

(Received 30 April 2008; published 12 September 2008; publisher error corrected 15 September 2008)

We report new measurements of the decays $B^+ \to \rho^+\gamma$, $B^0 \to \rho^0\gamma$, and $B^0 \to \omega\gamma$ using a data sample of 657×10^6 B meson pairs accumulated with the Belle detector at the KEKB e^+e^- collider. We measure branching fractions $\mathcal{B}(B^+ \to \rho^+\gamma) = (8.7^{+2.9+0.9}_{-2.7-1.1}) \times 10^{-7}$, $\mathcal{B}(B^0 \to \rho^0\gamma) = (7.8^{+1.7+0.9}_{-1.6-1.0}) \times 10^{-7}$, and $\mathcal{B}(B^0 \to \omega\gamma) = (4.0^{+1.9}_{-1.7} \pm 1.3) \times 10^{-7}$. We also report the isospin asymmetry $\Delta(\rho\gamma) = -0.48^{+0.21+0.08}_{-0.19-0.09}$ and the first measurement of the direct CP-violating asymmetry $A_{CP}(B^+ \to \rho^+\gamma) = -0.11 \pm 0.32 \pm 0.09$, where the first and second errors are statistical and systematic, respectively.

DOI: 10.1103/PhysRevLett.101.111801 PACS numbers: 13.20.He, 11.30.Er, 14.40.Nd, 14.65.Fy

The $b \to d\gamma$ process, which proceeds via a loop diagram [Fig. 1(a)] in the standard model (SM), provides a valuable tool to search for physics beyond the SM, since the loop diagram may also involve virtual heavy non-SM particles [1]. The process has been observed in the exclusive modes $B \to \rho\gamma$ and $B \to \omega\gamma$ by Belle [2] and *BABAR* [3]. Branching fractions for these modes have been used to constrain the ratio of Cabibbo-Kobayashi-Maskawa (CKM) matrix elements [4] $|V_{td}/V_{ts}|$; a non-SM effect may be observed as a deviation of $|V_{td}/V_{ts}|$ from the expectation based on measurements of other CKM matrix elements and unitarity of the matrix [5]. An additional contribution from an annihilation diagram [Fig. 1(b)] may induce a direct CP-violating asymmetry in $B^+ \to \rho^+\gamma$ and an isospin asymmetry between $B \to \rho\gamma$ modes; the latter can be used to constrain the CKM unitarity triangle angle ϕ_3 [6]. These quantities are also sensitive to physics beyond the SM [7]. In this Letter, we report new measurements of the $B \to \rho\gamma$ and $B \to \omega\gamma$ processes using a data sample of $(657 \pm 9) \times 10^6$ B meson pairs accumulated at the $\Upsilon(4S)$ resonance. With a data sample almost twice as large and an improved analysis procedure, these results supersede those in [2].

The data are obtained in e^+e^- annihilation at the KEKB energy-asymmetric (3.5 on 8 GeV) collider [8] and collected with the Belle detector [9]. The Belle detector includes a silicon vertex detector (SVD), a central drift chamber (CDC), aerogel threshold Cherenkov counters (ACC), time-of-flight (TOF) scintillation counters, and an electromagnetic calorimeter (ECL) comprised of CsI(Tl) crystals located inside a 1.5 T superconducting solenoid coil. An iron flux return located outside of the coil is instrumented to identify K_L^0 and muons.

We reconstruct three signal modes $B^+ \to \rho^+\gamma$, $B^0 \to \rho^0\gamma$, and $B^0 \to \omega\gamma$ and two control samples $B^+ \to K^{*+}\gamma$ and $B^0 \to K^{*0}\gamma$. Charge-conjugate modes are implicitly included unless otherwise stated. The following decay modes are used to reconstruct the intermediate states: $\rho^+ \to \pi^+\pi^0$, $\rho^0 \to \pi^+\pi^-$, $\omega \to \pi^+\pi^-\pi^0$, $K^{*+} \to K^+\pi^0$, $K^{*0} \to K^+\pi^-$, and $\pi^0 \to \gamma\gamma$.

Photon candidates are reconstructed from ECL energy clusters having a photonlike shape and no associated charged track. A photon with an $\Upsilon(4S)$ center-of-mass (c.m.) energy (E^*_γ) in the range $[1.8, 3.4]$ GeV is selected

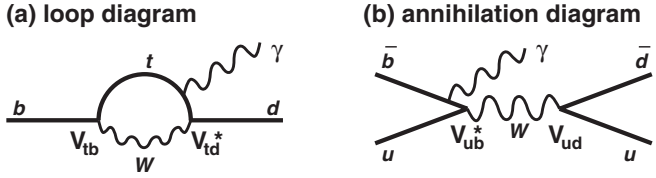

FIG. 1. (a) Loop diagram for $b \to d\gamma$ and (b) annihilation diagram, which contributes only to $B^+ \to \rho^+\gamma$.

as the primary photon candidate. Photons detected by the end cap ECL, which were excluded in the previous analysis, are also used. To suppress backgrounds from $\pi^0/\eta \to \gamma\gamma$ decays, we apply a veto algorithm based on the likelihood calculated for every photon pair consisting of the primary photon and another photon. We also reject the primary photon candidate if the ratio of the energy in the 3×3 crystal array, centered on the crystal with the maximum energy, to that in the 5×5 array is less than 0.95.

Neutral pions are formed from photon pairs with invariant masses within ± 16 MeV/c^2 ($\sim 3\sigma$) of the π^0 mass. We require the energy of each photon to be greater than 50 MeV and the cosine of the angle between the two photons in the laboratory frame to be greater than 0.58 (0.40) for the π^0 from ρ^+ (ω). The photon momenta are then recalculated with a π^0 mass constraint.

Charged pions and kaons are selected from tracks in the CDC and SVD. Each track is required to have a transverse momentum greater than 100 MeV/c and a distance of closest approach to the interaction point within 0.5 cm in radius and within ± 3.0 cm along the positron beam (z) axis. We use a likelihood ratio $\mathcal{L}_\pi/(\mathcal{L}_\pi + \mathcal{L}_K) < 0.3$ for pions and >0.6 for kaons, where the pion and kaon likelihoods $\mathcal{L}_\pi$ and $\mathcal{L}_K$ are determined from ACC, TOF, and CDC information. The criteria have efficiencies of 86%, 87%, and 89%, for a pion from ρ^+, ρ^0, and ω, respectively; the misidentification probability for a kaon is 8.3% (8.5%) for $\rho^+(\rho^0)$. Kaons for K^* candidates are selected with an efficiency of 85%. Invariant masses for the ρ, ω, and K^* candidates are required to be within windows of [640, 890], [760, 800], and [820, 970] MeV/c^2, respectively.

Candidate B mesons are reconstructed by combining a ρ or ω candidate with the primary photon and calculating two variables: the beam-energy constrained mass $M_{\rm bc} = \sqrt{(E^*_{\rm beam}/c^2)^2 - |\vec{p}^{\,*}_B/c|^2}$ and the energy difference $\Delta E = E^*_B - E^*_{\rm beam}$. Here $\vec{p}^{\,*}_B$ and E^*_B are the c.m. momentum and energy of the B candidate, respectively, and $E^*_{\rm beam}$ is the c.m. beam energy. To improve resolution, the magnitude of the photon momentum is replaced by $(E^*_{\rm beam} - E^*_{\rho/\omega})/c$ when the momentum $\vec{p}^{\,*}_B$ is calculated.

To optimize the event selection, we study Monte Carlo (MC) events in a signal box defined as $5.273\ {\rm GeV}/c^2 < M_{\rm bc} < 5.285\ {\rm GeV}/c^2$ and $|\Delta E| < 0.1$ GeV. For each signal mode, we choose selection criteria to maximize $N_S/\sqrt{N_S + N_B}$, where N_S and N_B are the expected signal and the sum of the background yields, respectively.

The dominant background arises from continuum events [$e^+e^- \to q\bar{q}(\gamma)$, $q = u, d, s, c$], where a random combination of a ρ or ω candidate with a photon forms a B candidate. We suppress this using a Fisher discriminant ($\mathcal{F}$) calculated from modified Fox-Wolfram moments [10] and other variables: i.e., the cosine of the polar angle ($\cos\theta^*_B$) of the B direction, the distance along the z axis (Δz) between the signal vertex and that of the rest of the event, and, in addition, $M_{\pi^+\pi^-\pi^0}$ and Dalitz plot variables for the $\omega\gamma$ mode. For each of these quantities, we construct likelihood distributions for signal and continuum events. The distributions are determined from MC samples.

From these likelihood distributions, we form likelihoods $\mathcal{L}_s$ and $\mathcal{L}_c$ for the signal and continuum background, respectively. In addition, we use a flavor-tagging quality variable r that indicates the level of confidence in the B-flavor determination as described in Ref. [11]. In the (r, $\mathcal{R}$) plane defined by the tagging quality r and the likelihood ratio $\mathcal{R} = \mathcal{L}_s/(\mathcal{L}_s + \mathcal{L}_c)$, the signal tends to populate the edges at $r = 1$ and $\mathcal{R} = 1$, while the continuum preferentially populates the edges at $r = 0$ and $\mathcal{R} = 0$. We divide the events into six bins of r (two bins between 0 and 0.5 and four bins between 0.5 and 1) and determine the minimum $\mathcal{R}$ requirement for each bin. In the $\rho^+\gamma$ mode, if the tagging-side flavor is the same as that of the signal side, we assign the events to the lowest bin $0 \le r < 0.25$. The $\mathcal{R}$ criteria reject 98% of the continuum background while retaining 35%, 51%, and 43% of the $\rho^0\gamma$, $\rho^+\gamma$, and $\omega\gamma$ signals, respectively. For the $K^{*+}\gamma$ ($K^{*0}\gamma$) mode, we use the criteria for the $\rho^+\gamma$ ($\rho^0\gamma$) mode.

We consider the following backgrounds from B decays: $B \to K^*\gamma$, other $B \to X_s\gamma$ processes, decays with a π^0/η ($B \to \rho\pi^0$, $\omega\pi^0$, $\rho\eta$, and $\omega\eta$), other charmless hadronic B decays, and $b \to c$ decay modes. The $B \to K^*\gamma$ background can mimic the $B \to \rho\gamma$ signal if the kaon from the K^* is misidentified as a pion. To suppress $B \to K^*\gamma$ events, we calculate $M_{K\pi}$, where the kaon mass is assigned to the charged pion candidate; for $\rho^0\gamma$, the lower of the two $M_{K\pi}$ values is taken (misassignment tends to give a higher $M_{K\pi}$). For the $\rho^+\gamma$ mode we reject the candidate if $M_{K\pi} < 0.90\ {\rm GeV}/c^2$, while for the $\rho^0\gamma$ mode we use $M_{K\pi}$ in the fit procedure to extract the signal (note: $M_{K\pi} > 0.92\ {\rm GeV}/c^2$ is required when optimizing selection criteria). The $b \to s\gamma$ modes ($B \to K^*\gamma$ and other $B \to X_s\gamma$ decays) contribute to the background when the ρ and ω candidates are formed from random combinations of particles. Decays with a π^0/η can mimic the signal if one of its daughter photons is not detected. To suppress this background, we reject the candidate if $|\cos\theta_{\rm hel}| > 0.80$, 0.75, and 0.83 for the $\rho^+\gamma$, $\rho^0\gamma$, and $\omega\gamma$ mode, respectively, where the helicity angle $\theta_{\rm hel}$ is the angle between the π^+ track (the normal to the ω decay plane) and the B momentum vector in the ρ (ω) rest frame. We study large MC samples and find no other distinctive hadronic B decay background sources.

The reconstruction efficiency for each mode is defined as the fraction of the signal remaining after all selection criteria are applied, where the signal yield is determined from a fit to the sum of the signal and continuum MC samples using the procedure described below. We take the pion identification efficiency from a data sample of $D^{*+} \to D^0\pi^+$, $D^0 \to K^-\pi^+$. The total efficiencies are listed in

TABLE I. Yield, significance with systematic uncertainty, efficiency, and branching fraction ($\mathcal{B}$) for each mode. The first and second errors in the yield and $\mathcal{B}$ are statistical and systematic, respectively. The subdecay $\mathcal{B}(\omega \to \pi^+\pi^-\pi^0)$ is included for the $\omega\gamma$ mode.

Mode	Yield	Significance	Efficiency (%)	$\mathcal{B}(10^{-7})$
$B^+ \to \rho^+\gamma$	$45.8^{+15.2+2.6}_{-14.5-3.9}$	3.3	8.03 ± 0.59	$8.7^{+2.9+0.9}_{-2.7-1.1}$
$B^0 \to \rho^0\gamma$	$75.7^{+16.8+5.1}_{-16.0-6.1}$	5.0	14.81 ± 0.95	$7.8^{+1.7+0.9}_{-1.6-1.0}$
$B^0 \to \omega\gamma$	$17.5^{+8.2+1.1}_{-7.4-1.0}$	2.6	6.58 ± 0.76	$4.0^{+1.9}_{-1.7} \pm 1.3$
$B \to \rho\gamma$	...	5.8	...	$12.1^{+2.4}_{-2.2} \pm 1.2$
$B \to (\rho, \omega)\gamma$	...	6.2	...	$11.4 \pm 2.0^{+1.0}_{-1.2}$

Table I. The systematic error in the efficiency is the quadratic sum of the following contributions, estimated using control samples: the uncertainty in the photon detection efficiency (2.4%) as measured in radiative Bhabha events; charged tracking efficiency (1.0% per track) from partially reconstructed $D^{*+} \to D^0\pi^+$, $D^0 \to K^0_S\pi^+\pi^-$, $K^0_S \to \pi^+(\pi^-)$; charged pion and kaon identification (0.5%–0.6% per track) from $D^{*+} \to D^0\pi^+$, $D^0 \to K^-\pi^+$; neutral pion detection (4.6%) from η decays to $\gamma\gamma$, $\pi^+\pi^-\pi^0$, and $3\pi^0$; and $\mathcal{R} - r$ and π^0/η veto requirements (2.0%–8.4%) from $B \to D\pi^-$ with $D^0 \to K^-\pi^+$, $K^0_S\omega$, and $D^+ \to K^-\pi^+\pi^+$.

We perform an unbinned extended maximum likelihood fit to $M_{\rm bc}$ and ΔE (and $M_{K\pi}$ for the $\rho^0\gamma$ mode) for candidates satisfying $|\Delta E| < 0.5$ GeV and $M_{\rm bc} > 5.2$ GeV$/c^2$. The fit is performed individually for the three $\rho\gamma/\omega\gamma$ signal modes and the two $K^*\gamma$ modes. We describe the events in the fit region using the sum of probability density functions for the signal, continuum, $K^*\gamma$ (for the $\rho\gamma$ modes only), and other background hypotheses. We use the distributions of MC events in histograms to model the $M_{\rm bc} - \Delta E$ shapes of B decay background components and the $M_{K\pi}$ shapes for all components.

The signal distribution for the $\rho^0\gamma$ and $K^{*0}\gamma$ modes is modeled as the product of a crystal ball line shape [12] in ΔE to reproduce the asymmetric ECL energy response, a Gaussian in $M_{\rm bc}$, and an MC histogram distribution for $M_{K\pi}$. For the $\rho^+\gamma$, $K^{*+}\gamma$, and $\omega\gamma$ modes, we use the product of a crystal ball line shape for ΔE and another crystal ball line shape for $M_{\rm bc}$. The signal parameters of $M_{\rm bc}$ and ΔE shapes for $K^*\gamma$ modes are determined from fitting the data; for the $\rho\gamma/\omega\gamma$ modes, they are taken from the MC samples and calibrated using the data/MC difference of the fits to the $K^{*+}\gamma$ and $K^{*0}\gamma$ samples for the modes with and without a neutral pion, respectively.

The continuum background component is modeled as the product of a linear function in ΔE, an ARGUS function [13] in $M_{\rm bc}$, and, for $\rho^0\gamma$, an MC histogram for $M_{K\pi}$. The continuum shape parameters and normalizations are mode-dependent and allowed to float.

There is significant $K^{*0}\gamma$ background in the $\rho^0\gamma$ sample. This background is modeled by the product of a two-dimensional $M_{\rm bc} - \Delta E$ histogram and an $M_{K\pi}$ histogram. Similarly, the $K^{*+}\gamma$ background for $\rho^+\gamma$ is modeled by a two-dimensional $M_{\rm bc} - \Delta E$ histogram. In both cases, the ΔE peak position is shifted from the $\rho\gamma$ signal peak; this offset is determined from fitting the MC histogram shape to a $K^*\gamma$ data sample in which the pion mass is assigned to kaons. The same $K^*\gamma$ sample together with the known kaon to pion misidentification probability is also used to determine the size of the $K^*\gamma$ background.

Other B decays are considered as an additional background component when we extract the signal yield. The levels of these backgrounds are fixed using known branching fractions or upper limits [14].

The systematic error in the signal yield due to the fitting procedure is estimated by varying each of the fixed parameters by $\pm 1\sigma$ and then taking the quadratic sum of the deviations in the branching fraction from the nominal value. The varied parameters are the signal shape parameters, branching fractions of the background components, ΔE shift of the $K^*\gamma$ component, and the kaon to pion misidentification probability determined from a control sample. The results of the fits are shown in Fig. 2 and listed in Table I.

The systematic error in the branching fraction has contributions from the efficiency, fitting, and the number of B meson pairs; we add these together in quadrature. The significance is defined as $\sqrt{-2\ln(\mathcal{L}_0/\mathcal{L}_{\rm max})}$, where $\mathcal{L}_{\rm max}$ ($\mathcal{L}_0$) is the value of the likelihood function when the signal yield is floated (set to zero). To include systematic uncertainty, the likelihood function from the fit is convolved with a Gaussian systematic error function.

Table I also lists combined branching fractions, which are calculated from the products of likelihoods from individual fits. We combine $\rho^+\gamma$ and $\rho^0\gamma$ modes (referred to as $\rho\gamma$) and three $\rho\gamma$ and $\omega\gamma$ modes [referred to as $(\rho, \omega)\gamma$] assuming a single branching fraction $\mathcal{B}(B \to \rho\gamma) \equiv \mathcal{B}[B \to (\rho, \omega)\gamma] \equiv \mathcal{B}(B^+ \to \rho^+\gamma) = 2\frac{\tau_{B^+}}{\tau_{B^0}}\mathcal{B}(B^0 \to \rho^0\gamma) = 2\frac{\tau_{B^+}}{\tau_{B^0}}\mathcal{B}(B^0 \to \omega\gamma)$ [15,16], where $\frac{\tau_{B^+}}{\tau_{B^0}} = 1.071 \pm 0.009$ [17]. The results are consistent with the previous measurements [2,3] and have smaller errors. They are also in agreement with SM predictions [6,16,18].

The ratios of the branching fractions of the $B \to \rho\gamma/\omega\gamma$ modes to those of the $B \to K^*\gamma$ modes can be related to $|V_{\rm td}/V_{\rm ts}|$ [6,16]. We calculate the ratios from likelihood curves of individual fits to the $B \to \rho\gamma/\omega\gamma$ and $B \to K^*\gamma$ samples. Systematic errors that do not cancel in the ratio are convolved into the likelihoods. We find

$$\frac{\mathcal{B}(B^0 \to \rho^0\gamma)}{\mathcal{B}(B^0 \to K^{*0}\gamma)} = 0.0206^{+0.0045+0.0014}_{-0.0043-0.0016}, \quad (1)$$

$$\frac{\mathcal{B}(B \to \rho\gamma)}{\mathcal{B}(B \to K^*\gamma)} = 0.0302^{+0.0060+0.0026}_{-0.0055-0.0028}, \quad (2)$$

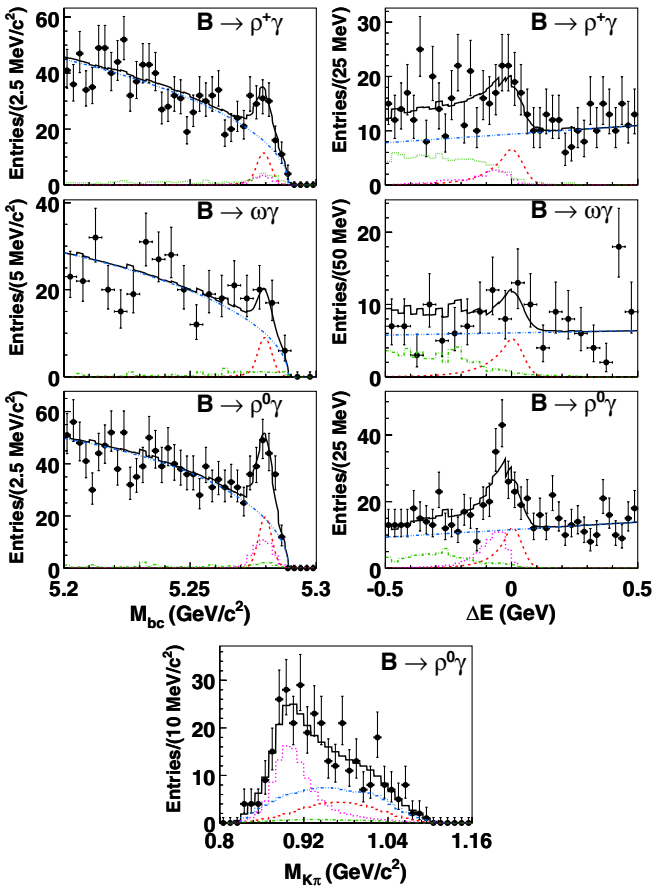

FIG. 2 (color online). Projections of the fit results to $M_{\rm bc}$ (in $|\Delta E| < 0.1$ GeV and $0.92\ {\rm GeV}/c^2 < M_{K\pi}$) and ΔE (in $5.273\ {\rm GeV}/c^2 < M_{\rm bc} < 5.285\ {\rm GeV}/c^2$ and $0.92\ {\rm GeV}/c^2 < M_{K\pi}$) and for $B^0 \to \rho^0\gamma$, $M_{K\pi}$. Curves show the signal (dashed, red), continuum (dotted-dotted-dashed, blue), $B \to K^*\gamma$ (dotted, magenta), other backgrounds (dashed-dotted, green), and the total fit result (solid).

$$\frac{\mathcal{B}(B \to (\rho,\omega)\gamma)}{\mathcal{B}(B \to K^*\gamma)} = 0.0284 \pm 0.0050^{+0.0027}_{-0.0029}, \qquad (3)$$

where the first and second errors are statistical and systematic, respectively.

Using the prescription in Ref. [6], Eq. (3), for example, gives $|V_{\rm td}/V_{\rm ts}| = 0.195^{+0.020}_{-0.019}({\rm exp}) \pm 0.015({\rm th})$. This is consistent with determinations from B^0_s mixing [14], which involve box diagrams rather than penguin loops. We also find $\mathcal{B}(B^+ \to K^{*+}\gamma) = (384 \pm 17) \times 10^{-7}$ and $\mathcal{B}(B^0 \to K^{*0}\gamma) = (378 \pm 8) \times 10^{-7}$ (statistical error only), in agreement with the world average.

From Table I, we calculate the isospin asymmetry $\Delta(\rho\gamma) = \frac{\tau_{B^0}}{2\tau_{B^+}}\mathcal{B}(B^+ \to \rho^+\gamma)/\mathcal{B}(B^0 \to \rho^0\gamma) - 1$ and find

$$\Delta(\rho\gamma) = -0.48^{+0.21+0.08}_{-0.19-0.09}. \qquad (4)$$

The result is in agreement with the previous measurement [3] and is only marginally consistent with the SM expectations [6,7].

We also calculate the direct CP-violating asymmetry $A_{CP}(B^+ \to \rho^+\gamma) = [N(\rho^-\gamma) - N(\rho^+\gamma)]/[N(\rho^-\gamma) + N(\rho^+\gamma)]$ using a simultaneous fit to $B^+ \to \rho^+\gamma$ and $B^- \to \rho^-\gamma$ data samples. We consider systematic errors due to the fitting procedure, asymmetries in the backgrounds, and possible detector bias estimated using a $B \to D\pi$ control sample. We use the measured asymmetries [14] for $B^+ \to K^{*+}\gamma$, $\rho^+\pi^0$, $\rho^+\eta$, and $B \to X_s\gamma$ and assume up to 100% asymmetry for other charmless hadronic B decays. We find

$$A_{CP}(B^+ \to \rho^+\gamma) = -0.11 \pm 0.32 \pm 0.09. \qquad (5)$$

The result is consistent with the SM predictions [6,16].

In conclusion, we present a new measurement of branching fractions for $B \to \rho\gamma$ and $B \to \omega\gamma$, a measurement of the isospin asymmetry, and the first measurement of the direct CP-violating asymmetry for $B^+ \to \rho^+\gamma$. The results are consistent with SM predictions. We improve the experimental precision on $|V_{\rm td}/V_{\rm ts}|$ determined from penguin loops, finding good agreement with the value determined from box diagrams [14].

We thank the KEKB group for excellent operation of the accelerator, the KEK cryogenics group for efficient solenoid operations, and the KEK computer group and the NII for valuable computing and SINET3 network support. We acknowledge support from MEXT and JSPS (Japan); ARC and DEST (Australia); NSFC and KIP of CAS (China); DST (India); MOEHRD, KOSEF, and KRF (Korea); KBN (Poland); MES and RFAAE (Russia); ARRS (Slovenia); SNSF (Switzerland); NSC and MOE (Taiwan); and DOE (USA).

[1] For example, A. Arhrib, C.-K. Chua, and W.-S. Hou, Eur. Phys. J. C **21**, 567 (2001); A. Ali and E. Lunghi, Eur. Phys. J. C **26**, 195 (2002); Z.-J. Xiao and C. Zhuang, Eur. Phys. J. C **33**, 349 (2004).
[2] D. Mohapatra *et al.* (Belle Collaboration), Phys. Rev. Lett. **96**, 221601 (2006).
[3] B. Aubert *et al.* (*BABAR* Collaboration), Phys. Rev. Lett. **98**, 151802 (2007).
[4] M. Kobayashi and T. Maskawa, Prog. Theor. Phys. **49**, 652 (1973); N. Cabibbo, Phys. Rev. Lett. **10**, 531 (1963).
[5] J. Charles *et al.* (CKM fitter group), Eur. Phys. J. C **41**, 1 (2005), and updates at http://ckmfitter.in2p3.fr; M. Bona *et al.* (UTfit Collaboration), J. High Energy Phys. 03 (2008) 049.
[6] P. Ball, G. W. Jones, and R. Zwicky, J. High Energy Phys. 04 (2006) 046; Phys. Rev. D **75**, 054004 (2007).
[7] A. Ali and E. Lunghi, Eur. Phys. J. C **26**, 195 (2002).
[8] S. Kurokawa and E. Kikutani, Nucl. Instrum. Methods Phys. Res., Sect. A **499**, 1 (2003), and other papers included in this volume.
[9] A. Abashian *et al.* (Belle Collaboration), Nucl. Instrum. Methods Phys. Res., Sect. A **479**, 117 (2002).
[10] S. H. Lee *et al.* (Belle Collaboration), Phys. Rev. Lett. **91**, 261801 (2003).

[11] H. Kakuno *et al.*, Nucl. Instrum. Methods Phys. Res., Sect. A **533**, 516 (2004).
[12] J. E. Gaiser *et al.* (Crystal Ball Collaboration), Phys. Rev. D **34**, 711 (1986).
[13] H. Albrecht *et al.* (ARGUS Collaboration), Phys. Lett. B **241**, 278 (1990).
[14] Heavy Flavor Averaging Group, winter 2006 results (http://www.slac.stanford.edu/xorg/hfag/).
[15] A. Ali, V. M. Braun, and H. Simma, Z. Phys. C **63**, 437 (1994).
[16] A. Ali and A. Parkhomenko, Eur. Phys. J. C **23**, 89 (2002); C.-D. Lu, M. Matsumori, A. I. Sanda, and M.-Z. Yang, Phys. Rev. D **72**, 094005 (2005); **73**, 039902(E) (2006).
[17] W.-M. Yao *et al.*, J. Phys. G **33**, 1 (2006).
[18] In addition to Ref. [16], see, e.g., S. Bosch and G. Buchalla, Nucl. Phys. **B621**, 459 (2002); T. Huang, Z. Li, and H. Zhang, J. Phys. G **25**, 1179 (1999); R. Fleischer and S. Recksiegel, Phys. Rev. D **71**, 051501 (R) (2005); M. Beneke, T. Feldmann, and D. Seidel, Eur. Phys. J. C **41**, 173 (2005).